Journal of Inorganic Biochemistry 141 (2014) 43–54

Contents lists available at ScienceDirect

Journal of Inorganic Biochemistry

journal homepage: www.elsevier.com/locate/jinorgbio

Synthesis and biological evaluation of 2-benzoylpyridine thiosemicarbazones in a dimeric system: Structure–activity relationship studies on their anti-proliferative and iron chelation efficacy

Adeline Y. Lukmantara [a,*], Danuta S. Kalinowski [b], Naresh Kumar [a,*], Des R. Richardson [b,**]

[a] School of Chemistry, University of New South Wales, Sydney, NSW 2052, Australia
[b] Molecular Pharmacology and Pathology Program, Department of Pathology and Bosch Institute, University of Sydney, Sydney, NSW, 2006, Australia

ARTICLE INFO

Article history:
Received 1 July 2014
Received in revised form 29 July 2014
Accepted 29 July 2014
Available online 7 August 2014

Keywords:
Thiosemicarbazone
Dimer
Lipophilicity
Iron

ABSTRACT

Thiosemicarbazone chelators represent an exciting class of biologically active compounds that show great potential as anti-tumor agents. Our previous studies demonstrated the potent anti-tumor activity of the 2′-benzoylpyridine thiosemicarbazone series. While extensive studies have been performed on monomeric thiosemicarbazone compounds, dimeric thiosemicarbazone chelators have received comparatively less attention. Thus, it was of interest to investigate the anti-proliferative activity and iron chelation efficacy of dimeric thiosemicarbazones. Two classes of dimeric thiosemicarbazones were designed and synthesized. The first class consisted of two benzoylpyridine-based thiosemicarbazone units connected *via* a hexane or dodecane alkyl bridge, while the second class of dimer consisted of two thiosemicarbazones attached to a 2,6-dibenzoylpyridine core. These dimeric ligands demonstrated greater anti-proliferative activity than the clinically used iron chelator, desferrioxamine. This study highlights the importance of optimal lipophilicity as a factor influencing the cytotoxicity and iron chelation efficacy of these chelators.

1. Introduction

Thiosemicarbazones have received significant attention from academia and the pharmaceutical industry over the past 50 years due to their rich biological activity [1]. These properties include potent anti-viral [2,3], anti-bacterial [4–6] and anti-cancer [7,8] efficacy. The α-(*N*)-heterocyclic class of thiosemicarbazones are derived from the Schiff base condensation reaction of thiosemicarbazides with aldehydes or ketones [1]. These ligands possess a conjugated *N*,*N*,*S* tridentate system that has been shown to be particularly important for their cytotoxic activity [9]. This effect is due to the fact that the N and S atoms are able to act as "soft" electron donors and chelate transition metal ions such as iron (Fe), copper and zinc to form cytotoxic metal complexes [5,9–11]. Such complexes can catalyze the formation of reactive oxygen species (ROS), including the hydroxyl radical, that can damage DNA and inhibit cellular proliferation [12–14].

Iron is an essential element for many cellular processes, including energy production, electron transport and DNA synthesis due to its role as a co-factor for proteins such as oxidases, cytochromes and ribonucleotide reductase [15–17]. While tumor cells and normal cells share highly similar biochemical processes, the higher requirement for Fe in cancerous tissues highlights the potential to target Fe and develop novel and selective chemotherapeutics [1,18–21]. The enhanced demand for Fe in tumor cells arises, at least in part, from the increased Fe requirement for enzymes that play critical roles in metabolism. These include ribonucleotide reductase (RR), an Fe-containing enzyme that catalyzes the conversion of ribonucleotides to deoxyribonucleotides, which is the rate-limiting step of DNA synthesis [1,15]. Hence, the inactivation of RR *via* Fe deprivation can inhibit DNA synthesis and cellular proliferation of tumor cells [22,23]. Furthermore, Fe chelation up-regulates the potent growth and metastasis suppressor, N-myc downstream regulated gene-1 (NDRG1), which suppresses multiple signaling pathways involved in tumorigenesis and metastasis [24–27].

Due to the importance of Fe in cancer cell proliferation, numerous Fe-chelating compounds have been investigated as potential anti-cancer agents [1]. For example, the thiosemicarbazone chelator, 3-aminopyridine 2-carboxaldehyde thiosemicarbazone (known as 3-AP or Triapine®), exhibited inhibition of L1210 leukemia cells *in vitro* and *in vivo* [15] and suppressed the growth of murine M109 lung carcinoma and human A2780 ovarian carcinoma xenografts in mice [20,28–31]. In fact, Triapine® was assessed in over 20 Phase I and II clinical trials and

* Corresponding authors at: Department of Chemistry, University of New South Wales, Australia. Tel.: +61 2 9385 4698.
** Correspondence to: D.R. Richardson, Department of Pathology and Bosch Institute, University of Sydney, Sydney 2006, Australia. Tel.: +61 2 9036 6548; fax: +61 2 9351 3429.
E-mail addresses: adeline.lukmantara@gmail.com (A.Y. Lukmantara), n.kumar@unsw.edu.au (N. Kumar), d.richardson@med.usyd.edu.au (D.R. Richardson).

http://dx.doi.org/10.1016/j.jinorgbio.2014.07.020
0162-0134/

recently has shown promising activity against cervical and vaginal cancers in combination with cisplatin and radiotherapy [32].

Other thiosemicarbazone-based chelators, including the 2′-benzoylpyridine thiosemicarbazone (BpT; **1**; Fig. 1), 2′-(3-nitrobenzoyl) pyridine thiosemicarbazone (NBpT; **2**; Fig. 1) and halogenated 2′-benzoylpyridine thiosemicarbazone (XBpT; **3**; Fig. 1) series have also shown potent and selective anti-tumor activity *in vitro* and *in vivo* (Fig. 1) [33,34]. In particular, 2′-benzoylpyridine 4,4-dimethyl-3-thiosemicarbazone (Bp44mT) showed potent anti-tumor activity upon oral administration to nude mice bearing human DMS-53 lung cancer xenografts and was very well tolerated [35]. Recently, we have also developed substituted 2′-benzoyl-6-methylpyridine thiosemicarbazones and 4-phenyl-substituted 2′-benzoylpyridine thiosemicarbazones that demonstrated selective anti-proliferative activity towards cancer cells *in vitro* [36,37].

While extensive studies have been performed on monomeric thiosemicarbazones compounds [1,33,36,37], dimeric thiosemicarbazone chelators have received comparatively less attention. Previous studies on the dimerization of thiazolones, quinones and aminopyridines, produced compounds with improved potency compared to the original monomers [38,39]. One of the most studied groups of dimeric thiosemicarbazones were the bis(thiosemicarbazone) series (**4**; Fig. 2). These ligands were composed of two thiosemicarbazone moieties connected by their imine nitrogens *via* a two-carbon bridge [40–42]. Earlier studies showed that bis(thiosemicarbazones) derived from dialdehydes, ketoaldehydes and diketones demonstrated anti-viral effects and anti-tumor activity against HeLa cells [42–45]. The copper(II), zinc(II), platinum(II) and palladium(II) complexes of bis(thiosemicarbazone) also possessed anti-neoplastic properties [43,45–54].

Due to the potential observed with bis(thiosemicarbazones), other dimeric structures were also investigated. Dithiosemicarbazones (**5**) are a class of dimeric thiosemicarbazones that consist of two thiosemicarbazone units connected by their amide nitrogen N(4) atoms *via* an aliphatic or aromatic spacer [41,42]. Notably, studies by Gingras et al. [55] have demonstrated that the dithiosemicarbazones (**5**) exhibited effective anti-fungal activity and *in vitro* anti-tumor activity [41,56]. Furthermore, the copper(II), platinum(II) and palladium(II) complexes of dithiosemicarbazones also showed anti-fungal, anti-bacterial and anti-tumor activities [40,41,56]. It was demonstrated that the dithiosemicarbazones formed 1:1 complexes with copper, in which the two thiocarbonyl groups of the symmetrical dithiosemicarbazone acted as donor atoms to a single copper ion [56].

Considering the promising anti-proliferative properties exhibited by our monomeric thiosemicarbazone chelators [33,34], it was of interest to investigate the effect of dimerization of these compounds on their biological activity. In fact, chelators of higher denticity generally form more stable Fe complexes than those chelators of lower denticity [1]. Additionally, dimers have demonstrated greater Fe chelation efficacy *in vivo* than their corresponding monomer [1]. Thus, it was important to further explore the biological activity of dimeric thiosemicarbazones derived from the potent BpT series [33]. In this study, two types of dimerization strategies were explored. In the first approach, we investigated the synthesis of dithiosemicarbazones containing two benzoylpyridine moieties connected *via* an alkyl bridge. Previous studies have employed a variety of linkers to connect iron chelator moieties, ranging from 2 to 11 atoms in length [1,40,41]. Thus, we synthesized dithiosemicarbazones using both a short (hexyl) and long (dodecyl) alkyl bridge to investigate the effect of the linker length on anti-proliferative activity and iron chelation efficacy. The second strategy employed 2,6-dibenzoylpyridine (**6**) as a core scaffold to connect together two thiosemicarbazide "tails". We herein report the synthesis of two novel dithiosemicarbazones and five 2,6-dibenzoylpyridine thiosemicarbazones (2,6-diBpT), and their ability to mobilize cellular Fe and inhibit Fe uptake from the Fe transport protein, transferrin (Tf).

Notably, this investigation represents the first attempt to combine two thiosemicarbazide "tails" into a single molecule using dibenzoylpyridine. In addition, it is also the first study to investigate the anti-proliferative activity of dimeric dibenzoylpyridine thiosemicarbazones. The current research highlights important structure–activity relationships regarding the structural requirements necessary for dimeric thiosemicarbazone-based chelators with potent anti-cancer activity.

2. Experimental

2.1. Chemicals

All commercially available reagents were purchased from Fluka, Sigma Aldrich, Alfa Aesar and Lancaster, and used without further purification. Desferrioxamine (DFO) was purchased from Novartis, Basel, Switzerland. All reactions requiring anhydrous conditions were performed under an argon/nitrogen atmosphere. Anhydrous solvents were obtained using a PureSolv MD Solvent Purification System.

2.2. Physical measurements

^{1}H and ^{13}C NMR spectra were obtained in the selected solvent on a Bruker DPX 300 spectrometer at the designated frequency and were internally referenced to the solvent peaks. Chemical shifts (δ) are in parts per million (ppm) downfield from tetramethylsilane (TMS) and the observed coupling constant (*J*) is in Hertz (Hz). Multiplicities are recorded as singlet (s), doublet (d), doublet of doublet (dd), doublet of triplet (dt), triplet (t), quarter (q), multiplet (m) and broad singlet (bs), where appropriate. Melting points were measured using a Mel-Temp melting point apparatus and are uncorrected. Microanalysis was performed on a Carlo Erba Elemental Analyzer EA 1108 at the Campbell Microanalytical Laboratory, University of Otago, New Zealand. Infrared spectra were recorded with a Thermo Nicolet 370 FTIR spectrometer as KBr disks. Ultraviolet visible spectra were recorded using a Varian Cary 100 Scan spectrometer in the designated solvents and data reported as wavelength (λ) in nm and extinction coefficient (ε) in $cm^{-1}\,M^{-1}$. Gravity column chromatography was carried out using Grace Davison LC60A 40–63 μm silica gel. Flash chromatography was done implementing Grace Davison LC60A 6–35 μm silica gel. Reactions were monitored using thin layer chromatography, performed on Merck DC aluminum plates coated with silica gel GF_{254}. Compounds were detected by short and long wavelength ultraviolet light. The log P_{calc} values were calculated using ChemBio Draw Ultra 13.0.

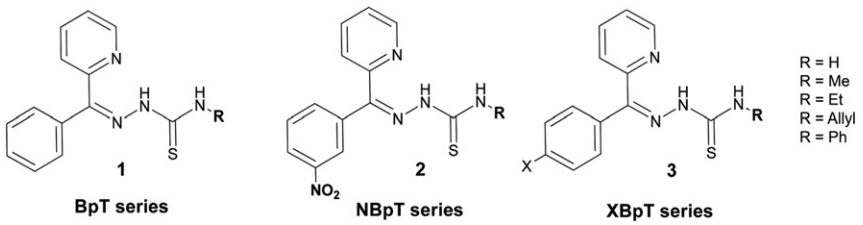

Fig. 1. General structures of the BpT, NBpT and XBpT series of thiosemicarbazone chelators.

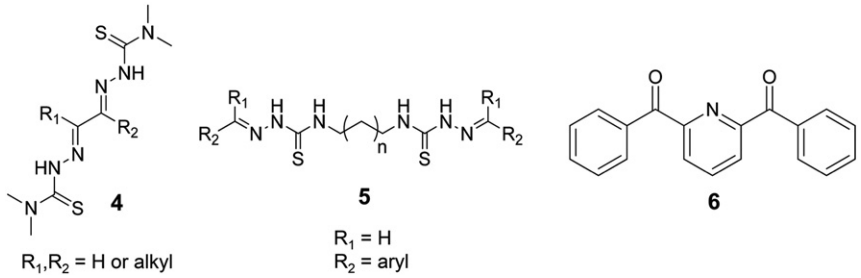

Fig. 2. General structures of bis(thiosemicarbazone) **4**, dithiosemicarbazone **5** and 2,6-dibenzoylpyridine **6**.

2.3. Single crystal X-ray diffraction studies

Single crystals for X-ray diffraction of (**16c**) were crystallized from EtOH or CH_2Cl_2/*n*-hexane. Suitable single crystals were selected under a polarizing microscope (Leica M165Z). These crystals were then loaded onto a MicroMount (MiTeGen, USA) consisting of a thin polymer tip with a wicking aperture. The X-ray diffraction measurements were carried out on a Bruker kappa-II CCD diffractometer at 150 K by using graphite-monochromated Mo-Kα radiation ($\lambda = 0.710723$ Å). The single crystals, mounted on the goniometer using cryo loops for intensity measurements, were coated with paraffin oil and then quickly transferred to the cold stream using an Oxford Cryo stream attachment. Symmetry-related absorption corrections using the program SADABS [57] were applied and the data were corrected for Lorentz and polarization effects using Bruker APEX2 software [58]. All structures were solved by direct methods and the full-matrix least-square refinements were carried out using SHELXL [59]. The non-hydrogen atoms were refined anisotropically. The molecular graphic was generated using mercury [60].

2.4. Electrochemistry

Cyclic voltammetry was performed using a BAS100B/W potentiostat. A glassy carbon working electrode, an aqueous Ag/AgCl reference, and a Pt wire auxiliary electrode were used. All complexes were at *ca.* 1 mM concentration in MeCN:H_2O (7:3) v/v. This solvent combination was used to ensure solubility of all compounds and has been utilized in our previous studies examining thiosemicarbazones [33,34]. The supporting electrolyte was Et_4NClO_4 (0.1 M), and the solutions were purged with nitrogen prior to measurement. All potentials are cited *versus* the normal hydrogen electrode (NHE) by addition of 196 mV to the potentials measured relative to the Ag/AgCl reference electrode.

2.5. Biological studies

2.5.1. Cell culture

The human SK-N-MC neuroepithelioma and MRC-5 fibroblast cell lines were obtained from the American Type Culture Collection (ATCC, Manassas, VA, USA) and were grown at 37 °C in a humidified atmosphere of 5% CO_2/95% air in an incubator [61]. All cell lines were grown in Eagle's minimum essential medium (MEM; Invitrogen, Mulgrave, Victoria, Australia) supplemented with 10% (v/v) fetal calf serum (Commonwealth Serum Laboratories, Melbourne, Victoria, Australia), 1% (v/v) non-essential amino acids (Invitrogen), 1% (v/v) sodium pyruvate (Invitrogen), 2 mM L-glutamine (Invitrogen), 100 μg/mL of streptomycin (Invitrogen), 100 U/mL penicillin (Invitrogen), and 0.28 μg/mL of fungizone (Squibb Pharmaceuticals, Montreal, Canada).

2.5.2. Preparation of Fe–Tf

Human serum Tf (Sigma-Aldrich, St. Louis, MO, USA) was labeled with ^{56}Fe or ^{59}Fe (Perkin-Elmer, Waltham, MA, USA) to produce $^{56}Fe_2$–Tf (^{56}Fe–Tf) or $^{59}Fe_2$–Tf (^{59}Fe–Tf), using previously reported methods [62,63].

2.5.3. Cellular proliferation assay

The effect of the chelators on cellular proliferation was determined by the MTT [1-(4,5-dimethylthiazol-2-yl-)-2,5-diphenyl tetrazolium] assay [33,61]. The SK-N-MC cell line was seeded in 96-well microtitre plates at 1.5×10^4 cells/well in medium containing human ^{56}Fe–Tf (1.25 μM) and chelators or their Fe complexes (0–25 μM). Chelators were freshly dissolved in DMSO as 10 mM stock solutions and diluted in medium so that the final [DMSO] < 0.5% (v/v). At this final concentration, DMSO had no effect on proliferation. Control samples contained medium with human ^{56}Fe–Tf (1.25 μM) without the ligands or complexes. After a 72 h incubation, 10 μL of MTT (5 mg/mL) was added to each well and the cells incubated for a further 2 h/37 °C. The cells were then lyzed with 100 μL of 10% SDS–50% isobutanol in 10 mM HCl. The plates were then read at 570 nm using a scanning multi-well spectrophotometer. The inhibitory concentration (IC_{50}) was defined as the chelator concentration necessary to reduce the absorbance to 50% of the untreated control.

2.5.4. Effect of chelators on ^{59}Fe efflux from SK-N-MC cells

Iron efflux experiments examining the ability of various chelators to mobilize ^{59}Fe from SK-N-MC cells were performed using established techniques [33,61]. Briefly, following prelabeling of cells with ^{59}Fe–Tf (0.75 μM) for 3 h/37 °C, the cell cultures were washed four times with ice-cold phosphate buffered saline (PBS). The cells were then subsequently incubated with either medium alone (control) or medium containing the chelator (25 μM) for 3 h/37 °C. The overlying media containing released ^{59}Fe was then separated from the cells using a Pasteur pipette. Radioactivity was measured in both the cell pellet and supernatant using a γ-scintillation counter (Wallace Wizard 3, Turku, Finland). In this study, the novel ligands were compared to the well characterized chelators, DFO, BpT, 2-benzoylpyridine 4-ethyl-3-thiosemicarbazone (Bp4eT) and di-2-pyridylketone 4,4-dimethyl-3-thiosemicarbazone (Dp44mT) [14,33,61].

2.5.5. Effect of chelators at preventing ^{59}Fe uptake from ^{59}Fe–Tf by SK-N-MC cells

The ability of the chelators to prevent cellular ^{59}Fe uptake from ^{59}Fe–Tf in SK-N-MC cells was examined and performed using standard procedures [14,33,61]. Briefly, cells were incubated with ^{59}Fe–Tf (0.75 μM) for 3 h/37 °C in the presence of medium alone (control) or in medium containing each of the chelators (25 μM). The cells were then washed four times with ice-cold PBS and internalized ^{59}Fe was determined by placing the culture plates on ice and incubating the cell monolayer with the protease, Pronase (1 mg/mL, Sigma) for 30 min/4 °C. The cells were then removed from the monolayer using a plastic spatula and centrifuged at 12,000 rpm/1 min. The supernatant represents membrane-bound, Pronase-sensitive ^{59}Fe, while the Pronase-insensitive fraction represents internalized ^{59}Fe [33,62,63]. In this assay, the novel chelators were compared to DFO and Dp44mT which are well characterized and

acted as positive controls [14,61]. Radioactivity was assessed as described above.

2.5.6. Statistical analysis

Experimental data were compared using Student's *t*-test. Results were expressed as mean ± SD (number of experiments).

2.6. Chemical synthesis

*2.6.1. 2,6-Dibenzoylpyridine (**6**)*

Excess thionyl chloride (25 mL) and two drops of DMF were added to 2,6-pyridinedicarboxylic acid (**14**; 5.0 g, 0.03 mol) and the mixture was heated at reflux for 2 h. The excess thionyl chloride was reduced and the crude residue was dissolved in benzene (50 mL). Then $AlCl_3$ (10 g, 0.07 mol) was added and the mixture was heated under reflux for 19 h. The resulting mixture was poured into a mixture of ice and concentrated HCl (32%, 50 mL), and extracted with diethyl ether (3 × 20 mL). The organic layer was washed with 1 M NaOH, dried over anhydrous Na_2SO_4 and evaporated under reduced pressure. The product was purified by flash chromatography using dichloromethane (DCM):*n*-hexane (7:3) to give dibenzoylpyridine (**6**) as a flaky-white powder (1.14 g, 93%). M.p. 108–110 °C, *lit.* [64] 109–110 °C; ^{1}H NMR (300 MHz, $CDCl_3$): δ 7.44–7.47 (m, 3H, ArH), 7.60–7.63 (m, 3H, ArH), 8.13–8.19 (m, 6H, ArH), and 8.32 (d, J = 8.1 Hz, 1H, ArH); ^{13}C NMR (75.6 MHz, $CDCl_3$): δ 126.92 (ArCH), 128.04 (4 × ArCH), 131.17 (4 × ArCH), 133.00 (2 × ArCH), 135.97 (ArCH), 138.32 (2 × ArC), 153.84 (2 × ArC), and 192.57 (2 × C═O).

*2.6.2. 4,4′-Hexanediyl-bis(thiosemicarbazide) (**8**)*

Carbon disulfide (CS_2; 4.5 mL, 7.5 mmol) was added to a mixture of 1,6-diaminohexane (**7**; 2.87 g, 25 mmol) and NaOH (2.08 g, 50 mmol) in water (25 mL). The mixture was stirred for 3.5 h at room temperature. Sodium chloroacetate (5.85 g, 50 mmol) was added and the resulting mixture was left to stir overnight at room temperature. The mixture was acidified with HCl (2 M, 8 mL), followed by the addition of excess hydrazine hydrate (12 mL). The solution was heated at reflux for 2 h and the precipitate that formed upon cooling was collected. The product was obtained as white crystals (1.55 g, 24%). M.p. 141–143 °C, *lit.* [65] 144–145 °C; ^{1}H NMR (300 MHz, DMSO-d_6): δ 1.24 (t, J = 6 Hz, 4H, CH_2), 1.47–1.51 (m, 4H, CH_2), 3.42 (t, J = 6 Hz, 4H, N–CH_2), 4.40 (bs, 4H, NH_2), 7.77 (s, 2H, NH), and 8.50 (s, 2H, NH); ^{13}C NMR (75.6 MHz, DMSO-d_6): δ 26.54 (2 × CH_2), 29.47 (2 × CH_2), 43.19 (2 × CH_2), and 181.48 (2 × C═S).

*2.6.3. N,N′-(Dodecane-1,12-diyl)bis(hydrazinecarbothioamide) (**10**)*

Carbon disulfide (CS_2, 8 mL) was added to a mixture of 1,12-diaminododecane (**9**; 3.32 g, 16.7 mmol) and NaOH (1.36 g, 33.3 mmol) in water (30 mL). The mixture was stirred for 6 h at room temperature. Sodium chloroacetate (5.0 g, 50 mmol) was added and the resulting mixture was left to stir overnight at room temperature. The mixture was acidified with HCl (2 M, 15 mL). The solution was heated at reflux for 2 h and the precipitate that formed upon cooling was collected. The product was obtained as an off white powder (2.30 g, 40%). M.p. 122–124 °C; ^{1}H NMR (300 MHz, DMSO-d_6): δ 1.22 (s, 16H, CH_2), 1.45–1.48 (m, 4H, CH_2), 3.39 (t, J = 9 Hz, 4H, N–CH_2), 4.39 (bs, 4H, NH_2), 7.77 (s, 2H, NH), and 8.49 (s, 2H, NH); ^{13}C NMR (75.6 MHz, DMSO-d_6): δ 26.32 (CH_2), 26.71 (CH_2), 29.21 (2 × 1CH_2), 29.40 (4 × CH_2), 29.48 (2 × CH_2), 43.21 (2 × CH_2), and 181.45 (2 × C═S). IR (KBr): υ_{max} 3243, 2915, 2849, 2366, 2062, 1604, 1566, 1501, 1470, 1413, 1364, 1288, 1260, 1216, 1148, 1095, 1058, 1048, 1028, 972, 934, 836, 775, 719, 632, 572, 499, 475, and 410; anal. calcd. for $C_{14}H_{32}N_6S_2$0.2CH_2Cl_2: C 46.66; H, 8.93; and N, 22.99. Found C, 46.60; H, 8.61; N, 22.70; High-resolution mass spectrometry (HRMS) (electrospray ionization; +ESI): Found m/z 371.2019 $[M + Na]^+$; $C_{14}H_{32}N_6S_2Na$ required 371.2028.

*2.6.4. General procedure for the synthesis of (**12**), (**13**) and (**16a–e**)*

The ketones were reacted with the appropriate thiosemicarbazide in ethanol (EtOH). A few drops of concentrated HCl (32%) were added as a catalyst and the solution was heated at reflux for 6 h. The resulting mixture was concentrated by rotary evaporation and the resulting precipitate was collected by vacuum filtration. The precipitate formed upon cooling was collected by vacuum filtration and recrystallized from EtOH.

*2.6.4.1. 2′-Benzoylpyridine-(1,6-hexane)-dithiosemicarbazone (**12**).* Compound (**12**) was synthesized following the general procedure above using 2-benzoylpyridine (**11**; 0.543 g, 3 mol) and 4,4′-hexanediyl-bis(thiosemicarbazide) (**8**; 0.413 g, 1.5 mol) in EtOH (25 mL) with 10 drops of conc. HCl. The compound was obtained as a yellow powder (655 mg, 39%). M.p. 206–208 °C; ^{1}H NMR (300 MHz, DMSO-d_6): δ 1.33 (s, 4H, CH_2), 1.63 (t, J = 6 Hz, 4H, CH_2), 3.42 (t, J = 6 Hz, 4H, CH_2), 7.35 (d, J = 9 Hz, 1H, ArH), 7.44–7.49 (m, 5H, ArH), 7.62–7.68 (m, 6H, ArH), 7.76–7.81 (m, 3H, ArH), 8.02 (dd, J = 9.0, 3.0 Hz, 1H, ArH), 8.24 (d, J = 9 Hz, 1H, ArH), 8.74–8.78 (m, 1H, ArH), 8.85 (s, 1H, NH), 9.06 (s, 1H, NH), 9.81 (s, 1H, NH), and 12.68 (s, 1H, NH); ^{13}C NMR (75.6 MHz, DMSO-d_6): δ 26.52 (2 × CH_2), 28.93 (2 × CH_2), 44.47 (2 × CH_2), 116.64 (ArCH), 118.76 (ArCH), 124.61 (ArCH), 125.31 (ArCH), 126.49 (ArCH), 128.76 (4 × ArCH), 129.28 (ArCH), 129.55 (4 × ArCH), 130.12 (ArCH), 130.80 (ArCH), 131.27 (2 × ArC), 138.76 (ArCH), 143.13 (2 × ArC), 149.14 (ArCH), 151.70 (2 × C═N), and 177.52 (2 × C═S); IR (KBr): υ_{max} 3346, 3236, 2925, 2859, 1615, 1561, 1472, 1359, 1316, 1159, 1132, 1079, 997, 974, 834, 793, 771, 733, 703, 649, 622, 606, and 494 cm^{-1}; UV–visible (UV–vis; MeOH): λ_{max} 260 nm (ε 12,800 cm^{-1} M^{-1}); anal. calcd. for $C_{32}H_{34}N_8S_2 \cdot 0.75CH_2Cl_2$: C, 59.74; H, 5.43; N, 17.02. Found C, 59.58; H, 5.78; and N, 17.36; HRMS (+ESI): Found m/z 595.2347 $[M + H]^+$; $C_{32}H_{25}N_8S_2$ required 595.2348.

*2.6.4.2. 2′-Benzoylpyridine-(1,12-dodecane)-dithiosemicarbazone (**13**).* Compound (**13**) was synthesized following the general procedure using 2-benzoylpyridine (**11**; 0.548 g, 3 mol) and *N,N′*-(dodecane-1,12-diyl)bis(hydrazinecarbothioamide) (**10**; 0.519 g, 1.5 mol) in EtOH (25 mL) with 8 drops of conc. HCl. The compound was obtained as a yellow powder (160 mg, 8%). M.p. 273–275 °C; ^{1}H NMR (300 MHz, DMSO-d_6): δ 1.22 (s, 16H, CH_2), 1.53 (t, J = 6 Hz, 4H, CH_2), 2.66–2.73 (m, 4H, CH_2), 7.22 (dd, J = 6.2 Hz, 2H, ArH), 7.38 (d, J = 3 Hz, 2H, ArH), 7.50–7.54 (m, 5H, ArH), 7.99 (d, J = 9 Hz, 2H, ArH), 8.09–8.12 (m, 5H, ArH), 8.27 (d, J = 6 Hz, 2H, ArH), 9.10 (s, 1H, NH), 9.12 (s, 1H, NH), 12.70 (s, 1H, NH), and 12.72 (s, 1H, NH); ^{13}C NMR (75.6 MHz, DMSO-d_6): δ 26.77 (2 × CH_2), 29.03 (2 × CH_2), 29.23 (4 × CH_2), 29.44 (2 × CH_2), 39.20 (2 × CH_2), 125.35 (2 × ArCH), 126.52 (2 × ArCH), 128.84 (4 × ArCH), 129.08 (ArCH), 129.39 (4 × ArCH), 129.64 (ArCH), 129.64 (ArCH), 137.41 (2 × ArC), 138.67 (ArCH), 143.32 (2 × ArC), 149.33 (2 × ArCH), 151.92 (2 × C═N), and 177.59 (2 × C═S); IR (KBr): υ_{max} 3399, 2924, 2849, 2522, 2361, 2046, 1604, 1527, 1494, 1471, 1397, 1299, 1257, 1225, 1207, 1164, 1147, 1047, 1036, 1014, 996, 939, 915, 825, 787, 767, 728, 699, 509, and 476 cm^{-1}; UV–vis (MeOH): λ_{max} 273 nm (ε 14,900 cm^{-1} M^{-1}), and 326 (26,500); anal. calcd. for $C_{38}H_{46}N_8S_2$.0.5CH_2Cl_2: C, 64.10; H, 6.57; and N, 15.53. Found C, 63.86; H, 6.15; N, 15.36; HRMS (+ESI): Found m/z 701.3478, $[M + Na]^+$ $C_{38}H_{46}N_8S_2Na$ required 701.3185.

*2.6.4.3. 2,6-Dibenzoylpyridine thiosemicarbazone (**16a**).* Compound (**16a**) was synthesized following the general procedure using 2,6-dibenzoylpyridine (**6**; 0.197 g, 0.696 mol) and thiosemicarbazide (**15a**; 0.159 g, 1.74 mol) in EtOH (25 mL) with 8 drops of conc. HCl. The compound was obtained as a yellow powder (253 mg, 85%). M.p. 223–228 °C; ^{1}H NMR (300 MHz, $CDCl_3$): δ 7.22 (dd, J = 1.2, 7.8 Hz, 1H, ArH), 7.33 (dd, J = 1.0, 8.1 Hz, 1H, ArH), 7.42 (dd, J = 1.8, 6.3 Hz, 1H, ArH), 7.48–7.51 (m, 3H, ArH), 7.54–7.58 (m, 4H, ArH), 7.64–7.73 (m, 3H, ArH), 7.77 (s, 2H, NH), 8.49 (s, 1H, NH), 8.78 (s, 1H, NH), and 13.88 (s, 2H, NH_2); ^{13}C NMR (75.6 MHz, $CDCl_3$): δ 125.38 (ArCH), 126.68 (ArCH), 128.61 (4 × ArCH), 129.13 (4 × ArCH), 130.52

(2 × ArCH), 130.90 (ArCH), 138.07 (2 × ArC), 148.40 (2 × ArC), 153.50 (2 × C═N), and 179.13 (2 × C═S); IR (KBr): υ_{max} 3261, 1584, 1474, 1265, 1084, 835, 769, and 702 cm^{-1}; UV–vis (MeOH): λ_{max} 211 nm (ε 113,720 cm^{-1} M^{-1}), 240 (88,488), 308 (105,526) and 313 (94,427); anal. calcd. for $C_{21}H_{19}N_7S_2 \cdot 0.2H_2O$: C, 57.70; H, 4.47; and N, 22.43. Found C, 57.76; H, 4.83; and N, 22.29; HRMS (+ESI): Found *m/z* 434.1213, $[M + H]^+$; $C_{21}H_{20}N_7S_2$ required 434.1177.

*2.6.4.4. 2,6-Dibenzoylpyridine 4-methyl-3-thiosemicarbazone (**16b**).* Compound (**16b**) was synthesized following the general procedure using 2,6-dibenzoylpyridine (**6**; 0.199 g, 0.696 mmol) in EtOH (25 mL), 4-methyl-3-thiosemicarbazide (**15b**; 0.181 g, 1.74 mmol) and 6 drops of conc. HCl and was obtained as a yellow powder (300 mg, 93%). M.p. 226–229 °C; ^{1}H NMR (300 MHz, $CDCl_3$): δ 3.31 (d, *J* = 4.8 Hz, 3H, CH_3), 3.35 (d, *J* = 4.8 Hz, 3H, CH_3), 7.12 (dd, *J* = 1.0, 8.1 Hz, 1H, ArH), 7.28 (dd, *J* = 1.0, 8.0 Hz, 1H, ArH), 7.41–7.43 (m, 2H, ArH), 7.48–7.51 (m, 3H, ArH), 7.54–7.57 (m, 2H, ArH), 7.62–7.74 (m, 4H, ArH), 7.86 (s, 1H, NH), 8.61 (s, 1H, NH), 8.77 (s, 1H, NH), and 13.89 (s, 1H, NH); ^{13}C NMR (75.6 MHz, $CDCl_3$): δ 31.13 (CH_3), 32.20 (CH_3), 125.18 (ArCH), 126.20 (ArCH), 128.69 (4 × ArCH), 129.13 (4 × ArCH), 130.46 (2 × ArCH), 130.91 (ArC), 137.59 (ArC), 137.87 (ArCH), 142.40 (ArC), 146.42 (ArC), 152.44 (C═N), 153.27 (C═N), 178.16 (C═S), and 178.91 (C═S); IR (KBr): υ_{max} 3473, 3361, 3281, 3041, 1541, 1475, 1218, 1105, 1041, 819, 772, and 699 cm^{-1}; UV–vis (MeOH): λ_{max} 212 nm (ε 247,000 cm^{-1} M^{-1}), 237 (166,000), 308 (215,000), and 315 (204,000); anal. calcd. for $C_{23}H_{23}N_7S_2$: C, 59.84; H, 5.02; and N, 21.24. Found C, 60.09; H, 5.00; and N, 21.21; HRMS (+ESI): Found *m/z* 484.1338, $[M + Na]^+$; $C_{23}H_{23}N_7S_2Na$ required 484.1354.

*2.6.4.5. 2,6-Dibenzoylpyridine 4-ethyl-3-thiosemicarbazone (**16c**).* Compound (**16c**) was synthesized following the general procedure using 2,6-dibenzoylpyridine (**6**; 0.151 g, 0.52 mmol) and 4-ethyl-3-thiosemicarbazide (**15c**; 0.159 g, 1.31 mmol) in EtOH (20 mL) with 8 drops of conc. HCl and was obtained as a yellow powder (230 mg, 89%). M.p. 234–237 °C; ^{1}H NMR (300 MHz, $CDCl_3$): δ 1.34 (t, *J* = 6.3 Hz, 6H, 2 × CH_3), 3.85 (q, *J* = 6.3 Hz, 4H, 2 × CH_2), 7.17 (dd, *J* = 1.2, 7.8 Hz, 1H, ArH), 7.27 (dd, *J* = 1.0, 8.1 Hz, 1H, ArH), 7.40 (dd, *J* = 1.8, 9.3 Hz, 1H, ArH), 7.48–7.52 (m, 4H, ArH), 7.53–7.58 (m, 3H, ArH), 7.61–7.75 (m, 3H, ArH), 7.82 (s, 1H, NH), 8.64 (s, 1H, NH), 8.72 (s, 1H, NH), and 13.69 (s, 1H, NH); ^{13}C NMR (75.6 MHz, $CDCl_3$): δ 14.45 (CH_3), 14.49 (CH_3), 39.29 (CH_2), 40.01 (CH_2), 124.97 (ArCH), 126.13 (ArCH), 128.71 (4 × ArCH), 129.10 (ArCH), 129.22 (2 × ArCH), 130.43 (2 × ArCH), 130.89 (ArC), 137.60 (ArC), 142.40 (ArC), 146.51 (ArC), 152.36 (C═N), 153.41 (C═N), 177.15 (C═S), and 177.88 (C═S); IR (KBr): υ_{max} 3290, 3054, 2973, 1525, 1460, 1279, 1199, 1107, 949, 813, and 701 cm^{-1}; UV–vis (MeOH): λ_{max} 217 nm (ε 99,100 cm^{-1} M^{-1}), 238 (89,700), 308 (92,500), 313 (77,000), 323 (76,000) and 352 (50,100); anal. calcd. for $C_{25}H_{27}N_7S_2$: C, 61.32; H, 5.56; and N, 20.02. Found C, 61.38; H, 5.49; and N, 19.74; HRMS (+ESI): Found *m/z* 512.1653, $[M + Na]^+$; $C_{25}H_{27}N_7S_2Na$ required 512.1667.

*2.6.4.6. 2,6-Dibenzoylpyridine 4-allyl-3-thiosemicarbazone (**16d**).* Compound (**16d**) was synthesized following the general procedure using 2,6-dibenzoylpyridine (**6**; 0.102 g, 0.348 mmol) and 4-allyl-3-thiosemicarbazide (**15d**; 0.119 g, 0.912 mmol) in EtOH (20 mL) with 6 drops of conc. HCl and was obtained as a yellow solid (153 mg, 84%). M.p. 177–180 °C; ^{1}H NMR (300 MHz, $CDCl_3$): δ 4.41–4.50 (m, 4H, CH_2), 5.20–5.39 (m, 4H, CH_2), 5.80–6.10 (m, 2H, CH), 7.23 (dd, *J* = 8.1, 2.2 Hz, 1H, ArH), 7.43 (dd, *J* = 1.8, 8.1 Hz, 1H, ArH), 7.46–7.52 (m, 4H, ArH), 7.53–7.57 (m, 3H, ArH), 7.61–7.71 (m, 4H, ArH), 7.75 (s, 1H, NH), 7.89 (s, 1H, NH), 8.79 (s, 1H, NH), and 13.72 (s, 1H, NH); ^{13}C NMR (75.6 MHz, $CDCl_3$): δ 46.71 (CH_2), 47.19 (CH_2), 116.71 (CH_2), 116.94 (CH_2), 124.92 (ArCH), 126.23 (ArCH), 128.70 (4 × ArCH), 129.20 (4 × ArCH), 129.42 (ArCH), 130.71 (2 × ArCH), 133.46 (CH), 133.60 (CH), 137.50 (ArC), 137.89 (ArC), 142.61 (ArC), 146.81 (ArC), 152.29 (C═N), 153.40 (C═N), 177.78 (C═S), and 178.24 (C═S); IR (KBr): υ_{max} 3286, 3069, 1637, 1524, 1274, 1189, 1109, 926, 827, 770, and 696 cm^{-1}; UV–vis (MeOH): λ_{max} 215 nm (ε 101,000 cm^{-1} M^{-1}), 237 (76,400), 308 (91,000) and 316 (81,000); anal. calcd. for $C_{27}H_{27}N_7S_2$: C, 63.13; H, 5.30; and N, 19.09. Found C, 63.24; H, 5.11; and N, 18.89; HRMS (+ESI): Found *m/z* 514.1829, $[M + H]^+$; $C_{27}H_{28}N_7S_2$ required 514.1803.

*2.6.4.7. 2,6-Dibenzoylpyridine 4-phenyl-3-thiosemicarbazone (**16e**).* Compound (**16e**) was synthesized following the general procedure using 2,6-dibenzoylpyridine (**6**; 0.198 g, 0.696 mmol) and 4-phenyl-3-thiosemicarbazide (**15e**; 0.288 g, 1.74 mmol) in EtOH (20 mL) with 6 drops of conc. HCl and was obtained as a yellow powder (219 mg, 54%). M.p. 239–243 °C; ^{1}H NMR (300 MHz, $CDCl_3$): δ 7.18 (dd, *J* = 1.0, 8.1 Hz, 2H, ArH), 7.28 (dd, *J* = 1.0, 8.1 Hz, 2H, ArH), 7.42 (dd, *J* = 1.8, 8.1 Hz, 2H, ArH), 7.48–7.52 (m, 5H, ArH), 7.53–7.58 (m, 4H, ArH), 7.61–7.70 (m, 6H, ArH), 7.73 (d, *J* = 8.1 Hz, 2H, ArH), 7.80 (s, 1H, NH), 8.72 (s, 1H, NH), and 13.70 (s, 1H, NH); ^{13}C NMR (75.6 MHz, $CDCl_3$): δ 126.12 (4 × ArCH), 128.71 (4 × ArCH), 129.11 (4 × ArCH), 129.36 (4 × ArCH), 130.66 (2 × ArCH), 130.90 (2 × ArCH), 137.62 (ArCH), 137.83 (2 × ArC), 142.38 (2 × ArC), 146.48 (2 × ArC), 152.37 (C═N), 153.42 (C═N), 177.16 (C═S), and 177.89 (C═S); IR (KBr): υ_{max} 3288, 2973, 1529, 1459, 1277, 1199, 1107, 951, 811, and 699 cm^{-1}; UV–vis (MeOH): λ_{max} 319 nm (ε 57,800 cm^{-1} M^{-1}); anal. calcd. for $C_{33}H_{27}N_7S_2 \cdot 3H_2O$: C, 61.95; H, 5.20; and N, 15.32. Found C, 61.69; H, 5.37; and N, 15.43; HRMS (+ESI): Found *m/z* 586.1805, $[M + H]^+$; $C_{33}H_{28}N_7S_2$ required 586.1803.

2.6.5. General procedure of the synthesis of dimeric [Fe^{III}(BpT)] complexes

The desired thiosemicarbazone chelator (3.5 mmol) was dissolved in absolute EtOH (15 mL). A few drops of Et_3N were added to the solution followed by the addition of $Fe(ClO_4)_3 \cdot 6H_2O$ (1.7 mmol). The mixture was gently refluxed overnight, and after cooling, the dark brown precipitate was filtered and washed with EtOH.

*2.6.5.1. [Fe(Bp-(1,6-hexane)diT)]$ClO_4 \cdot 0.5H_2O$ (**17**).* Dark brown solid (19.2 mg, 35%); anal. calcd. for $C_{32}H_{32}FeClN_8O_4S_2 \cdot 0.5H_2O$: C, 50.77; H, 4.39; and N, 14.80. Found: C, 50.93; H, 4.67; and N, 14.68. HRMS (+ESI): Found *m/z* 648.1520, $[M]^+$; $C_{32}H_{32}FeN_8S_2$ required 648.1541.

*2.6.5.2. [Fe(Bp-(1,12-dodecane)diT)]ClO_4 (**18**).* Dark brown solid (5.4 mg, 13%); anal. calcd. for $C_{38}H_{48}FeClN_8O_4S_2$: C, 54.58; H, 5.79; and N, 13.40. Found: C, 54.63; H, 6.01; and N, 13.46. HRMS (+ESI): Found *m/z* 736.2752, $[M]^+$; $C_{38}H_{48}FeN_8S_2$ required 736.2793.

*2.6.5.3. [Fe(2,6-diBpT)$_2$]$4H_2O$ (**19a**).* Dark brown solid (33.9 mg, 32%); anal. calcd. for $C_{42}H_{36}FeN_{14}S_4 \cdot 4H_2O$: C, 50.80; H, 4.47; and N, 19.75. Found: C, 51.18; H, 4.10; and N, 19.93. HRMS (+ESI): Found *m/z* 920.1458, $[M]^+$; $C_{42}H_{36}FeN_{14}S_4$ required 920.1479.

*2.6.5.4. [Fe(2,6-diBp4mT)$_2$]ClO_4 (**19b**).* Dark brown solid (47 mg, 44%); anal. calcd. for $C_{46}H_{44}FeClN_{14}O_4S_4$: C, 51.32; H, 4.12; and N, 18.22. Found: C, 51.03; H, 4.62; and N, 18.10. HRMS (+ESI): Found *m/z* 976.2316, $[M]^+$; $C_{46}H_{44}FeN_{14}S_4$ required 976.2105.

*2.6.5.5. [Fe(2,6-diBp4eT)$_2$]$ClO_4 \cdot 7H_2O$ (**19c**).* Dark brown solid (24.3 mg, 23%); anal. calcd. for $C_{50}H_{52}ClFeN_{14}O_4S_4 \cdot 7H_2O$: C, 47.63; H, 5.44; and N, 15.55. Found: C, 47.96; H, 5.47; and N, 15.37. HRMS (+ESI): Found *m/z* 1033.3249, $[M]^+$; $C_{50}H_{52}FeN_{14}S_4$ required 1033.2765.

*2.6.5.6. [Fe(2,6-diBp4aT)$_2$]$ClO_4 \cdot 5H_2O$ (**19d**).* Dark brown solid (13.2 mg, 13%); anal. calcd. for $C_{53}H_{52}ClFeN_{14}O_4S_4 \cdot 5H_2O$: C, 50.96; H, 5.07; and N, 15.41. Found: C, 50.79; H, 5.14; and N, 15.03. HRMS (+ESI): Found *m/z* 1080.2581, $[M]^+$; $C_{53}H_{52}FeN_{14}S_4$ required 1080.2731.

*2.6.5.7. [Fe(2,6-diBp4pT)$_2$]$ClO_4 \cdot 8H_2O$ (**19e**).* Dark brown solid (8.2 mg, 11%); anal. calcd. for $C_{66}H_{58}ClFeN_{14}O_4S_4 \cdot 8H_2O$: C, 53.75; H, 5.06; and

N, 13.30. Found: C, 53.97; H, 5.13; and N, 13.19. HRMS (+ESI): Found *m/z* 1230.3221, $[M]^+$; $C_{53}H_{52}FeN_{14}S_4$ required 1230.3201.

3. Results and discussion

3.1. Synthesis and characterization

The synthesis of dithiosemicarbazides was performed using a literature method [47] in which CS_2 was reacted with 1,6-diaminohexane (**7**) or 1,12-diaminododecane (**9**) in the presence of aqueous NaOH. Sodium chloroacetate was then added and the reaction was stirred overnight. This was followed by the addition of $H_2NNH_2 \cdot H_2O$ to yield the dithiosemicarbazides (**8**) and (**10**) (Scheme 1).

The structures of the products were confirmed by NMR spectroscopy. In the ^{1}H NMR spectrum of the symmetrical molecule (**8**) in d_6-DMSO, triplets at δ 1.24, 1.47 and 3.39 corresponded to the $-CH_2-$ groups of the hexane bridge, while a broad singlet at δ 4.40 corresponded to the $-NH_2$ protons. The NH protons adjacent to the C═S group appeared at δ 7.77 and δ 8.50. In the ^{13}C NMR spectrum, the appearance of a peak at δ 181.5 indicated the presence of the C═S carbon atoms. In comparison to the monomeric thiosemicarbazides, the dithiosemicarbazides showed lower solubility and could not be dissolved in $CDCl_3$.

The synthesis of the dithiosemicarbazones was conducted using established Schiff base condensation methodology [33,36,37], in which 1 equivalent of dithiosemicarbazide (**8**) or (**10**) was reacted with 2 equivalents of benzoylpyridine (**11**) in EtOH using HCl as catalyst. The reaction was heated at reflux overnight and yielded the novel dithiosemicarbazones (**12**) and (**13**) as yellow crystalline solids (Scheme 2).

In the ^{1}H NMR spectrum of (**12**) in d_6-DMSO, broad triplets at δ 1.04, 1.33 and 3.57 corresponded to the CH_2 groups of the hexane linker. The successful incorporation of the benzoylpyridine rings was indicated by the appearance of aromatic doublets and multiplet peaks at δ 7.22–8.86. Moreover, the NH protons of the hydrazide proton that are known to hydrogen bond to the pyridine nitrogen [13,33], appeared downfield at δ 12.68. Finally, the ^{13}C NMR spectrum of (**12**) revealed the appearance of C═N carbon atom at 154.88 and the C═S carbon atom resonance at δ 177.5.

To generate the 2,6-diBpT analogs, 2,6-dibenzoylpyridine (**6**) was first synthesized using a method reported by Lash et al. [64] in which pyridine dicarboxylic acid (**14**) was treated with excess thionyl chloride and catalytic DMF to afford a diacyl chloride intermediate. The diacyl chloride was then reacted with benzene under Friedel–Crafts acylation conditions to give 2,6-dibenzoylpyridine (**6**) as a white solid (Scheme 3). The crude solid was purified by flash chromatography using *n*-hexane:DCM (3:7) to yield the target compound in 93% yield.

The structure of 2,6-dibenzoylpyridine (**6**) was confirmed by ^{1}H NMR spectroscopy, which was consistent with reported literature values [64]. The presence of additional doublets and multiplets in the aromatic region δ 7.29–8.92 were indicative of the two phenyl rings that had been incorporated into the molecule. In the ^{13}C NMR spectrum, the presence of a peak at δ 192.6 confirmed the presence of the two C═O carbon atoms.

Similarly, the 2,6-diBpT series of ligands were synthesized through Schiff base condensation methodology [33,36,37] by reacting 2 equivalents of the thiosemicarbazide analogs (**15a**–**e**) with 1 equivalent of 2,6-dibenzoylpyridine in EtOH using concentrated HCl as a catalyst (Scheme 4). The desired 2,6-diBpT analogs (**16a**–**e**) were obtained in 54–93% yields.

Identification of compounds (**16a**–**e**) was performed using ^{1}H NMR and ^{13}C NMR spectroscopy. The ^{1}H NMR spectrum of compound (**16c**) in $CDCl_3$ was characteristic for all the symmetrical dimeric thiosemicarbazones (**16a**–**e**). A triplet at δ 1.34 and a quartet at δ 3.85 corresponded to the presence of the CH_3 and CH_2 protons of the ethyl group, respectively. The aromatic protons H2′/H2″, H3′/H3″, H4′/H4″, H5′/H5″ and H6′/H6″ (see Scheme 4 for numbering) appeared between δ 7.48 and 7.75. The characteristic hydrogen-bonded NH protons appeared as a singlet at δ 13.69. Further structural confirmation of (**16c**) was obtained from the ^{13}C NMR spectrum, where the disappearance of the peak at δ 192.6 along with the appearance of peaks at δ 152.4 and δ 153.4 indicated that the C═O bonds in the molecule had been replaced with C═N bonds. Furthermore, the new peaks at δ 177.2 and δ 177.9 corresponded to the presence of C═S carbon atoms in the structure. The presence of two C═N and two C═S peaks at very close values was attributed to the formation of both *E* and *Z* isomers at the imine bond.

3.2. Synthesis of iron complexes of dimeric thiosemicarbazone

Previous studies on the complexation of thiosemicarbazones and aroylhydrazones with metal ions have demonstrated marked changes in the biological activity of the ligands [13,33,34,66]. Therefore, the Fe complexes of the dimeric thiosemicarbazones were synthesized in order to investigate the anti-proliferative activity in comparison with the free ligands. The Fe^{III} complexes of the dimeric thiosemicarbazones were synthesized and characterized. The dimeric thiosemicarbazones were dissolved in EtOH with the addition of few drops of Et_3N as a catalyst, followed by the addition of $Fe(ClO_4)_3 \cdot 6H_2O$. The reactions were heated and the resulting precipitate was filtered and washed with EtOH.

All the synthesized complexes were brown in color and air stable, signifying the formation of Fe^{III} complexes. Moreover, these compounds were only soluble in polar solvents such as dimethylformamide (DMF) or DMSO. The analytical data showed that the 2,6-diBpT ligands (**16a**–**e**) formed 2:1 ligand:metal complexes, while the dithiosemicarbazones (**12** and **13**) formed 1:1 ligand:metal complexes. This result suggests that the dithiosemicarbazones (**12** and **13**) act as hexadentate ligands, using their pyridyl nitrogens, imine nitrogens and thiocarbonyl sulfurs as donor atoms.

3.3. Crystal structure of ligand 16c

Final confirmation of the structure of the 2,6-diBpT analogs was provided through X-ray crystallography (Fig. 3). In the ORTEP view of the ligand (**16c**), there are three intra-molecular N–H…N hydrogen bonds, as well as three intra-molecular C–H…S contacts which have also been observed with the monomer ligands [33,36]. The most significant interactions are N3–H4N…S, C15–H15A…S and C24–H24A…S, which maintain the overall planarity of the molecule. Hydrogen bonding S…H distances are in the range of 2.68–2.86 Å, while hydrogen bonding H…N distances are in the range of 0.98–2.31 Å. The H (N–H…N) angle varies from 107 to 134°, which are similar to the values observed in the previously synthesized BpT ligands [33].

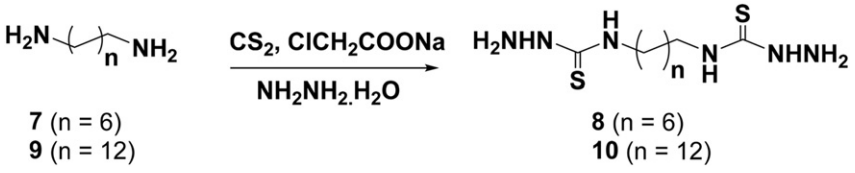

Scheme 1. Reagents and conditions: i) $NaOH/H_2O$, CS_2, $ClCH_2COONa$, ii) $NH_2NH_2 \cdot H_2O$.

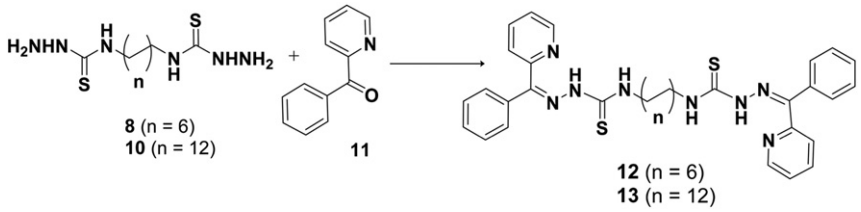

Scheme 2. Reagents and conditions: EtOH, HCl, reflux, 8 h and 90 °C.

3.4. Electrochemistry

The electrochemical properties of the Fe complexes of the dimeric thiosemicarbazones were examined *via* cyclic voltammetry to determine the potential of the complexes to undergo redox cycling in a physiological context [13,33,34]. Previous studies on thiosemicarbazone-based chelators have shown a correlation between anti-proliferative activity and the capability to undergo Fenton chemistry upon complexation with intracellular Fe [13,33]. Hence, it was important to investigate the electrochemical properties of the Fe complexes formed by these dimeric systems.

The Fe complex of 2′-benzoylpyridine-(1,6-hexane)-dithiosemicarbazone (**17**) underwent reversible $Fe^{III/II}$ redox coupling in MeCN:H_2O (7:3) at +131 mV *vs* the NHE (Table 1). This represented an anodic shift of 32 mV compared with the monomeric 2′-benzoylpyridine 4-ethyl-3-thiosemicarbazone [$Fe(Bp4eT)_2$] complex, which had a redox potential of +99 mV *vs.* the NHE [33]. Investigation of the redox potential of the Fe complex 2′-benzoylpyridine-(1,12-dodecane)-dithiosemicarbazone (**18**) proved to be problematic due to its low solubility in the solvent combination used. Notably, the solvent combination implemented herein (*i.e.*, MeCN:H_2O; 7:3) was utilized as it has shown to be optimal for dissolving other thiosemicarbazones that our group has studied [33,34].

The redox potential of the Fe complexes of the 2,6-diBpT analogs (**19a–d**) were measured and exhibited totally reversible $Fe^{III/II}$ couples in MeCN:H_2O (7:3), with significant cathodic shifts of 57–184 mV relative to the parent BpT chelators [33] (Table 1). Of the Fe complexes of the novel chelators **19a–d**, [$Fe(2,6\text{-diBpT})_2$] (**19a**) had the highest redox potential of +123 mV *vs.* the NHE. In contrast, [$Fe(2,6\text{-diBp4mT})_2$] (**19b**), [$Fe(2,6\text{-diBp4eT})_2$] (**19c**) and [$Fe(2,6\text{-diBp4aT})_2$] (**19d**) had lower redox potential values of +56, −4.5 and +18 mV *vs.* the NHE, respectively (Table 1). Again, the redox potential of [$Fe(2,6\text{-diBp4pT})_2$] (**19e**) could not be measured due to its low solubility. When comparing the redox potentials of the two classes of dimeric thiosemicarbazones, the Fe complex of dithiosemicarbazone (**17**) showed an anodic shift of 11–135.5 mV compared to the Fe complexes of the 2,6-diBpT series (**19a–d**) (Table 1).

The reversible electrochemical behavior of the Fe complexes suggests that the novel chelators could be able to assist the generation of intracellular ROS and undergo reversible redox cycling, which is known to play a key role in the anti-proliferative activity of thiosemicarbazones against tumor cells [13,14,67,68].

3.5. Biological studies

3.5.1. Anti-proliferative activity against tumor cells

The anti-proliferative activity of the dimeric thiosemicarbazones was examined in SK-N-MC neuroepithelioma cells using the MTT assay (Table 2). This cell-type was utilized as it has been widely used in our laboratory to examine the anti-proliferative activity of a range of related monomeric thiosemicarbazones [33,34]. Hence, the results obtained could be readily compared to these previous data. The anti-proliferative activity of 2′-benzoylpyridine-(1,6-hexane)-dithiosemicarbazone (**12**), 2′-benzoylpyridine-(1,12-dodecane)-dithiosemicarbazone (**13**) and the 2,6-dibenzoylpyridine thiosemicarbazones (**16a–e**) were compared with the clinically used positive control chelator, DFO, and the monomeric thiosemicarbazones of the BpT series [33].

The 7 novel dimeric chelators displayed moderate anti-proliferative activity against SK-N-MC cells, with IC_{50} values ranging from 0.31 to 10.64 μM, and were more potent than DFO (IC_{50}: 21.06 μM; Table 2). The most potent dimeric chelators, namely 2,6-diBpT (**16a**) and the dithiosemicarbazone (**12**), exhibited IC_{50} values of 0.31 ± 0.009 and 0.33 ± 0.049 μM, respectively, and were significantly ($p < 0.001$) more potent than DFO. On the other hand, 2,6-diBp4pT (**16e**) was the least active of all the dimeric thiosemicarbazones ($IC_{50} > 6.25$ μM). In general, in comparison to the dimeric thiosemicarbazones, their corresponding monomeric chelators showed far more potent activity in SK-N-MC cells, with IC_{50} values of 0.002–4.66 μM [33] (Table 2). A notable exception to this observation was 2,6-diBpT (**16a**), which showed approximately 15-fold greater anti-proliferative activity than its monomeric counterpart, BpT (Table 2).

It has been demonstrated that lipophilicity of chelators plays an important role in determining their anti-proliferative activity as its influences membrane permeability [61]. Optimal lipophilicity enables chelators to permeate the membrane lipid bilayer without retention. In this study, the less potent chelators **13** and **16b–d** had log P_{calc} values of 4.84–6.69 (Table 2). Notably, the least active compounds, namely **13** and **16e** (R = Ph), possessed the highest log P_{calc} values of 9.19 and 8.17, respectively. The correlation between lipophilicity and anti-proliferative efficacy (Fig. 4) is consistent with previous studies, where thiosemicarbazones with the most potent anti-proliferative activity had log P_{calc} values between 3.5 and 4.5 [13,33,34,69]. In light of these observations, the more hydrophobic chelators, **13** and **16e**, could become trapped in the cell membrane, preventing entrance into the cell and their ability to target Fe [34,69]. This indicates that optimal lipophilicity is crucial for enhancing the anti-proliferative activity of these ligands.

3.5.2. Anti-proliferative activity of Fe complexes of dimeric thiosemicarbazones against tumor cells

Previous studies have shown that complexation of the chelators with Fe can result in changes in the anti-proliferative activity [33,66,70]. Thus, the effect of Fe complexation of the dimeric chelators on anti-proliferative activity was examined using SK-N-MC neuroepithelioma cells (Table 2). The results showed the Fe complexes of compounds **12**, **13**, and **16a–16d**, namely the Fe complexes **17**, **18** and **19a–d**, respectively, were significantly ($p < 0.005$) less potent than their corresponding free ligands, with the Fe complexes **17** and **18** showing IC_{50} values greater than 6.25 μM. In fact, most of the Fe complexes, especially **19a–d**, showed a 2- to 20-fold decrease in anti-proliferative activity compared to the free chelators, which was consistent with previous findings [33,66,70]. Both the ligand **16e** and its Fe complex **19e** did not

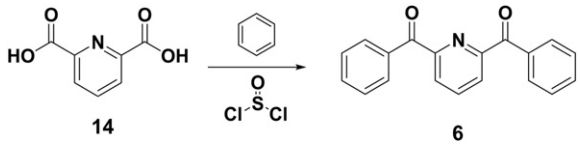

Scheme 3. Reagents and conditions: i) $SOCl_2$, DMF, ii) benzene, $AlCl_3$.

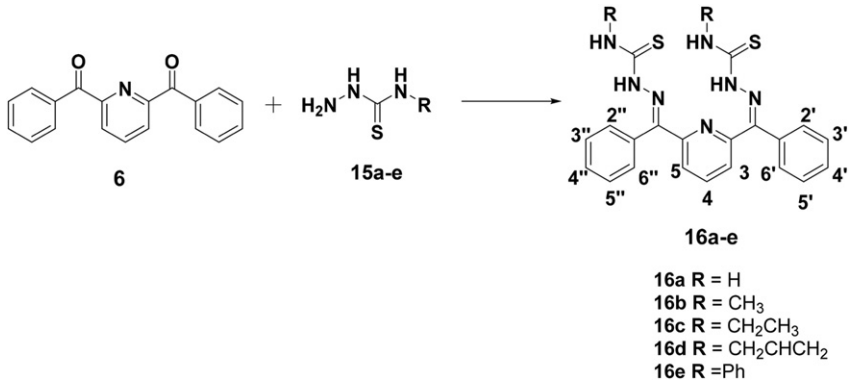

Scheme 4. Reagents and conditions: EtOH, conc. HCl, reflux, 8 h and 95 °C.

show any marked anti-proliferative effects (IC_{50} > 6.25 μM; Table 2). The lower potency of the Fe complexes may be attributed to their inability to chelate intracellular Fe that is required for DNA synthesis and proliferation [13,33]. In addition, due to the enhanced lipophilicity of the complexes relative to the ligands [71], they may partition into membranes to a greater extent and prevent entrance into the cytosol, which could reduce their efficacy.

3.5.3. Anti-proliferative activity against mortal cells

The selectivity of the novel dimeric thiosemicarbazones was evaluated by assessing their toxicity towards mortal human MRC-5 fibroblasts relative to the neoplastic SK-N-MC cell-type (Table 2). Interestingly, the mortal cells were significantly ($p < 0.001$) less sensitive to the novel chelators, **12** and **16a**–**d**, compared to neoplastic cells. The dimeric chelators exhibited a 3- to 20-fold decrease in anti-proliferative activity against mortal cells, with all compounds showing IC_{50} values greater than 5.32 μM. Notably, the dimer **16a**, was the most potent chelator against SK-N-MC cells and also showed the highest selectivity when compared to the anti-proliferative activity observed with MRC-5 cells. It is well known that cancer cells require higher levels of Fe than normal cells due to their rapid proliferation [1]. This arises from the increased Fe requirement for metabolic enzymes, such as RR, that is up-regulated in cancer cells [1]. Hence, the selective anti-proliferative activity of the chelators towards neoplastic cells suggests the presence of a "therapeutic window" in which tumor cells can be selectively targeted with less effect against mortal cells.

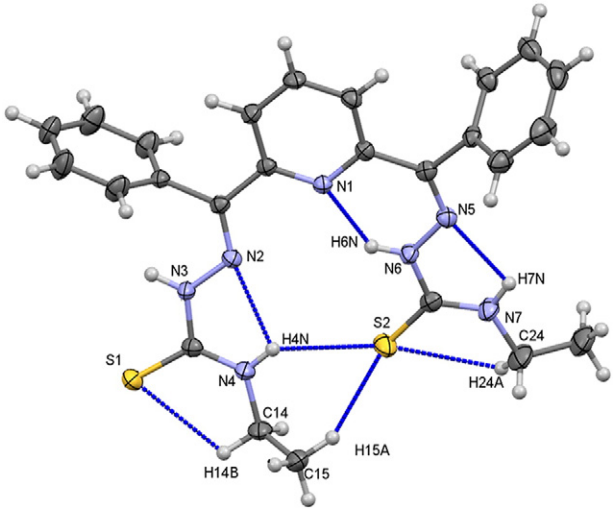

Fig. 3. ORTEP representation of **16c** (thermal ellipsoids are drawn at 50% probability level).

3.5.4. Mobilization of cellular ^{59}Fe from cells

The ability of chelators to effectively mobilize intracellular Fe plays a crucial role in their anti-proliferative activity [61]. Therefore, the ability of the dimeric thiosemicarbazone-based chelators to mobilize intracellular ^{59}Fe from prelabeled SK-N-MC neuroepithelioma cells was evaluated. The release of intracellular ^{59}Fe by the ligands (25 μM) was compared to the positive controls, DFO, Dp44mT, BpT and Bp4eT, which have been previously characterized in this cell-type [33].

As shown previously, DFO exhibited limited ability to efflux cellular ^{59}Fe [61,68], releasing only 14 ± 1% of intracellular ^{59}Fe, compared to 7 ± 1% of intracellular ^{59}Fe mobilized by control medium alone (Fig. 5a). On the other hand, the ligands used as positive controls, namely Dp44mT, BpT and Bp4eT, mediated the release of 36 ± 1%, 35 ± 1% and 33 ± 1% of intracellular ^{59}Fe, respectively. The high activity of these latter ligands at mobilizing ^{59}Fe was in good agreement with previous studies [33]. Of the 2,6-diBpT chelators, compound **16a** showed the greatest ability to mediate intracellular ^{59}Fe efflux (28 ± 1%), while compounds **16b**–**e** released 15–24% of cellular ^{59}Fe. Among the dithiosemicarbazones, compound **12** mediated the release of 18 ± 1% of intracellular ^{59}Fe, while compound **13** released only 4 ± 1% of intracellular ^{59}Fe (Fig. 5a). This latter result suggested that because of its very high lipophilicity (log P_{calc} 9.19), **13** became trapped within the cell membrane, restricting efflux of intracellular ^{59}Fe to a lesser extent than the control.

The Fe mobilization efficacy of the novel dimeric thiosemicarbazones was found to correlate with their anti-proliferative activity ($R^2 = 0.803$, Fig. 5b), with the most cytotoxic chelator **16a** having the highest ^{59}Fe mobilization activity, while the least cytotoxic chelator **13**, resulted in limited ^{59}Fe mobilization. Plotting ^{59}Fe mobilization against log P_{calc} values showed a linear relationship ($R^2 = 0.813$; Fig. 5c), indicating that chelators with increased lipophilicity are least efficient in mediating ^{59}Fe mobilization. The relatively low Fe mobilization efficacy of the dimeric thiosemicarbazones compared to monomeric chelators such as

Table 1
The $Fe^{III/II}$ redox potentials of the dimeric thiosemicarbazones in 7:3, MeCN:H_2O.

Ligand	$Fe^{III/II}$ redox potential (mV *vs* NHE)
[Fe(BpT)$_2$]	+120[a]
[Fe(Bp4mT)$_2$]	+108[a]
[Fe(Bp4eT)$_2$]	+99[a]
[Fe(Bp4aT)$_2$]	+117[a]
[Fe(Bp4pT)$_2$]	+180[a]
[Fe(Bp-1,6-hexanediT)] (**17**)	+131
[Fe(Bp-1,12-dodecanediT)] (**18**)	ND
[Fe(2,6-diBpT)$_2$] (**19a**)	+123
[Fe(2,6-diBp4mT)$_2$] (**19b**)	+56
[Fe(2,6-diBp4eT)$_2$] (**19c**)	−4.5
[Fe(2,6-diBp4aT)$_2$] (**19d**)	+18
[Fe(2,6-diBp4pT)$_2$] (**19e**)	ND

[a] $Fe^{III/II}$ redox potentials previously reported [33].

Table 2
IC_{50} values of the dimeric thiosemicarbazones and their Fe^{III} complexes at inhibiting the growth of SK-N-MC neuroepithelioma cells and mortal MRC-5 fibroblasts as determined by the MTT assay. Log P_{calc} values of the ligands were calculated using ChemBio Draw software.

Chelators	Log P_{calc}	Average IC50 values (μM)		
		Free ligands		Fe^{III} complex
		SK-N-MC	MRC-5	SK-N-MC
DFO		21.74 ± 2.58	>25[a]	>25[b]
BpT[c]	1.92	4.66 ± 1.59	>6.25	1.17 ± 0.17
Bp4mT[c]	0.74	0.004 ± 0.002	>6.25	0.013 ± 0.001
Bp4eT[c]	4.01	0.002 ± 0.001	>6.25	0.40 ± 0.06
Bp4aT[c]	2.69	0.004 ± 0.004	>6.25	0.34 ± 0.06
Bp4pT[c]	1.92	0.005 ± 0.002	1.86 ± 1.77	0.17 ± 0.01
Bp-1,6-hexanediT (**12**)	6.69	0.33 ± 0.049	5.32 ± 1.59	>6.25
Bp-1,12-dodecanediT (**13**)	9.19	10.64 ± 1.374	>12.5	>12.5
2,6-diBpT (**16a**)	3.8	0.31 ± 0.009	>6.25	0.77 ± 0.15
2,6-diBp4mT (**16b**)	4.84	1.98 ± 0.39	>6.25	4.79 ± 1.90
2,6-diBp4eT (**16c**)	5.51	1.65 ± 0.24	>6.25	>6.25
2,6-diBp4aT (**16d**)	6.51	1.50 ± 0.76	>6.25	3.83 ± 1.78
2,6-diBp4pT (**16e**)	8.17	>6.25	>6.25	>6.25

[a] Denotes data previously obtained in our laboratory using MRC-5 cells and DFO [14].
[b] Denotes data previously obtained in our laboratory using SK-N-MC cells and the DFO Fe complex [13].
[c] Denotes data previously obtained in our laboratory using SK-N-MC and MRC-5 cells and the appropriate monomeric thiosemicarbazones [33].

Dp44mT, BpT and Bp4eT, could be explained by their high lipophilicity and molecular size, which could inhibit their ability to transverse the cell membrane resulting in membrane sequestration [13,33].

3.5.5. Inhibition of cellular ^{59}Fe uptake from ^{59}Fe–Tf

The anti-proliferative activity of chelators is known to involve both the release of intracellular Fe from cells, as well as the inhibition of Fe uptake from Tf [13,33,61]. Thus, the ability of the novel dimeric thiosemicarbazones (25 μM) to inhibit internalized ^{59}Fe uptake from ^{59}Fe–Tf was assessed using SK-N-MC neuroepithelioma cells, and the results were compared to the well characterized positive controls, DFO, Dp44mT, BpT and Bp4eT [33].

As shown in previous studies [61], the ability of DFO to inhibit ^{59}Fe uptake was poor, with uptake reduced to only 96 ± 1% of the control, while Dp44mT, BpT and Bp4eT decreased ^{59}Fe uptake to 4 ± 1%, 11 ± 1% and 16 ± 1% of the control, respectively (Fig. 6a). All of the dimeric thiosemicarbazones were significantly ($p < 0.05$) more effective than DFO at inhibiting ^{59}Fe uptake from ^{59}Fe–Tf. The 2,6-diBpT chelators, **16a–e**, inhibited ^{59}Fe uptake to 33–58% of the control, which was significantly ($p < 0.01$) more effective than DFO, but markedly less effective than the monomeric thiosemicarbazones (Fig. 6a). Among the dimeric thiosemicarbazones, a correlation was evident where the most effective chelators in the ^{59}Fe efflux assay were also the most active at inhibiting ^{59}Fe uptake ($R^2 = 0.884$; Fig. 6b). For example, 2,6-diBpT, **16a**, which was the best of the dimeric ligands to induce ^{59}Fe efflux (Fig. 5a), was also the most effective dimeric ligand at reducing ^{59}Fe uptake to 33 ± 1% of the control (Fig. 6a).

The dithiosemicarbazones, **12** and **13**, were relatively less effective than the 2,6-diBpT series of ligands, and reduced ^{59}Fe uptake to 62 ± 1% and 81 ± 1% of the control, respectively. In addition, a linear relationship between inhibition of ^{59}Fe uptake and lipophilicity was observed ($R^2 = 0.716$, Fig. 6c), indicating that high lipophilicity led to decreased ^{59}Fe uptake efficacy. Again, this could be due to the highly lipophilic ligands becoming trapped in the cell membrane which would decrease their ability to enter the cell and reduce the incorporation of Fe from Tf. A relationship was also observed between the anti-proliferative activity (IC_{50}) and the ability of the ligands to inhibit ^{59}Fe uptake ($R^2 = 0.918$; Fig. 6d). In this latter case, the chelators with the greatest efficacy at decreasing ^{59}Fe uptake were also the most effective at inhibiting proliferation.

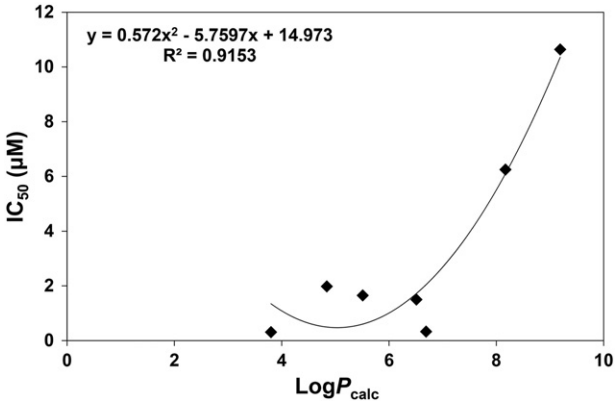

Fig. 4. Relationship between the anti-proliferative activity (IC_{50}) and lipophilicity (log P_{calc}) of the dimeric thiosemicarbazones.

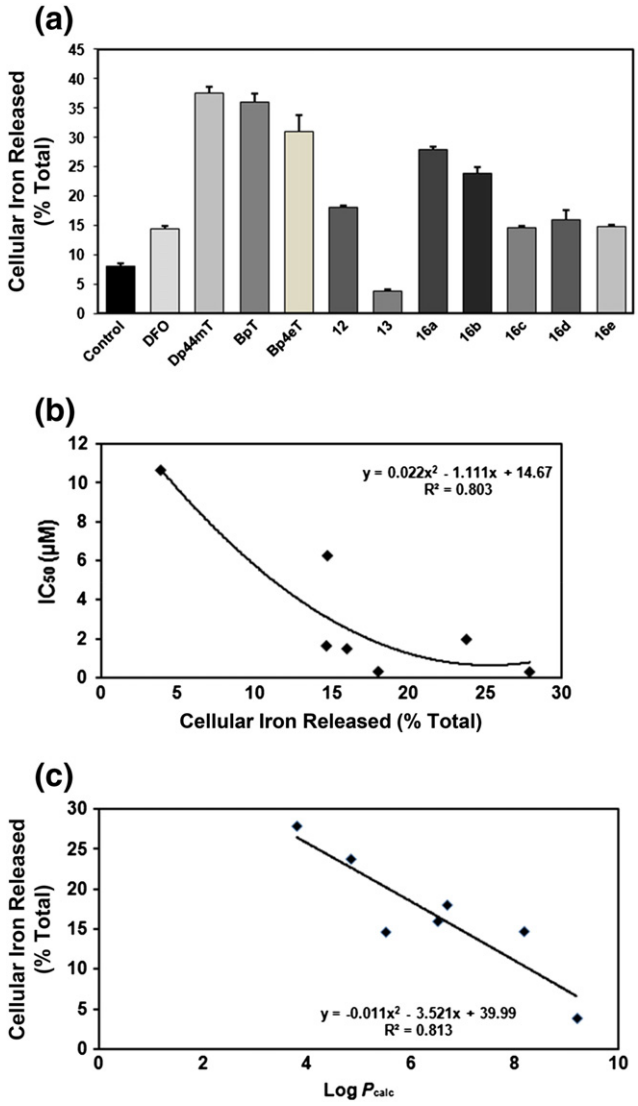

Fig. 5. (A) The effect of the chelators on ^{59}Fe mobilization from prelabeled SK-N-MC neuroepithelioma cells. Results are mean ± SD of 3 experiments with 3 determinations in each experiment. (B) The relationship between ^{59}Fe mobilization efficacy of the novel dimeric thiosemicarbazones and their anti-proliferative activity. (C) The relationship between ^{59}Fe mobilization in SK-N-MC cells and lipophilicity (log P_{calc}) of the dimeric chelators.

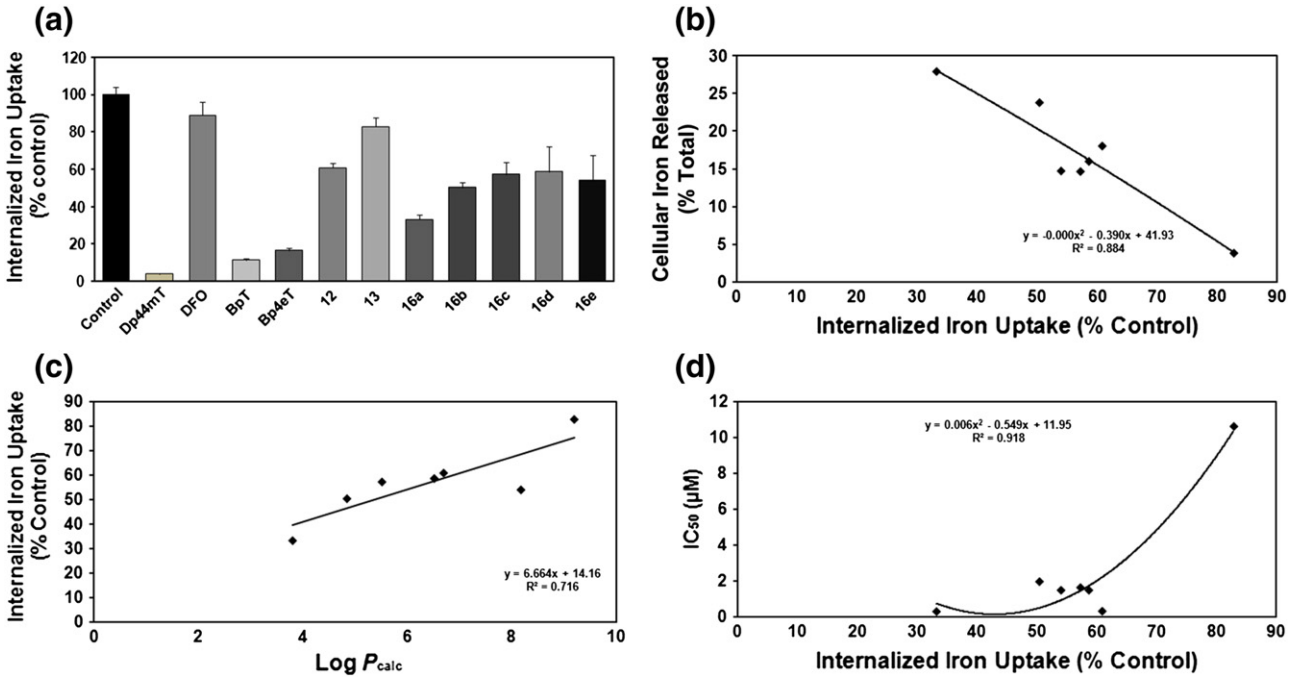

Fig. 6. (A) The effect of the dimeric chelators at inhibiting ^{59}Fe uptake from ^{59}Fe–Tf by SK-N-MC neuroepithelioma cells. Results are mean ± SD of 3 experiments with 3 determinations in each experiment. (B) A correlation was evident where the most effective dimeric thiosemicarbazones in the ^{59}Fe efflux assay were also the most active at inhibiting internalized ^{59}Fe uptake by SK-N-MC cells. (C) The relationship between ^{59}Fe uptake by SK-N-MC cells and lipophilicity (log P_{calc}) of the dimeric thiosemicarbazones. (D) The relationship between anti-proliferative activity (IC_{50}) and the ability of the dimeric ligands to inhibit ^{59}Fe uptake from ^{59}Fe–Tf by SK-N-MC cells.

Taken together, the ^{59}Fe efflux and ^{59}Fe uptake results above indicated that the dimeric chelators with a shorter hydrocarbon linker or lower molecular weight exhibited higher ^{59}Fe mobilization efficacy, as well as higher inhibition of ^{59}Fe uptake from ^{59}Fe–Tf. This correlation is demonstrated by the observation that chelator **16a** (R═H) was more active in terms of both ^{59}Fe mobilization (Fig. 5a) and inhibition of ^{59}Fe uptake (Fig. 6a) compared to analogs **16b**–**e** that contain larger alkyl, alkenyl or phenyl substituents. Similarly, dithiosemicarbazone **12** containing a hexyl linker showed higher ^{59}Fe chelation efficiency compared to dithiosemicarbazone **13**, which possesses a dodecyl bridge. The correlation between molecular weight and ability to inhibit ^{59}Fe uptake is shown in Fig. 7a, and demonstrates that as the molecular weight of the dimeric ligand increases, the ability to inhibit ^{59}Fe uptake decreases ($R^2 = 0.763$). In addition, Fig. 7b demonstrates that there is a decrease in ^{59}Fe efflux from SK-N-MC cells as the molecular weight of the dimeric thiosemicarbazone increases ($R^2 = 0.745$). This observation can be explained by the fact that when the chelators are too large or hydrophobic, they do not permeate the cell membrane effectively, or become trapped within the lipophilic environment of the membrane. Hence, molecular size and lipophilicity are important factors that play crucial roles in facilitating chelator entrance into cells and chelation of intracellular Fe.

4. Conclusions

The current investigation examined the effect of dimerization of thiosemicarbazones on their Fe chelation and anti-proliferative activity. The results have also highlighted important structure–activity relationships towards understanding the potential of dimeric thiosemicarbazones to act as effective anti-proliferative agents for the treatment of cancer. In this study, two new classes of dimeric thiosemicarbazones were synthesized and characterized. The first type of dimer was composed of two benzoylpyridine-based thiosemicarbazone units joined *via* a hexane or dodecane alkyl bridge, while the second class of dimer consisted of two thiosemicarbazone tails attached to a 2,6-dibenzoylpyridine core. To the best of our

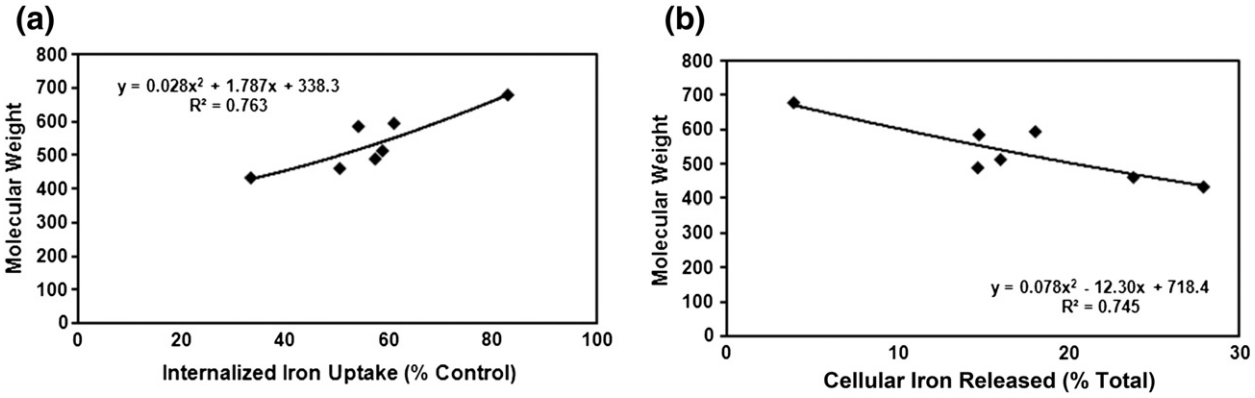

Fig. 7. The relationship between the molecular weight (MW) of the dimeric thiosemicarbazones and (A) ^{59}Fe uptake from ^{59}Fe–Tf by SK-N-MC cells and (B) ^{59}Fe release from SK-N-MC cells.

knowledge, these types of dimeric thiosemicarbazone have not yet been reported in the literature.

2′-Benzoylpyridine-(1,6-hexane)-dithiosemicarbazone (**12**) and the 2,6-diBpT analogs (**16a**–**e**), demonstrated moderate anti-proliferative activity against SK-N-MC cells, being more potent than the well-known chelator, DFO. The dimeric chelators also showed marked selectivity for tumor cells over normal cells. Additionally, the 2,6-diBpT analogs, **16a**–**e**, and dithiosemicarbazone **12** were able to mobilize intracellular ^{59}Fe and inhibit ^{59}Fe uptake with equal or greater efficacy than DFO. Significantly, the most cytotoxic chelator **16a** was also the most effective at mobilizing ^{59}Fe and preventing ^{59}Fe uptake (reduced to 33% of control). Moreover, the reversible electrochemical behavior of the Fe complexes of most of the dimeric thiosemicarbazones occurred in a range accessible to intracellular oxidants and reductants. These studies suggested the Fe(III) complexes may participate in redox cycling and ROS generation. The analytical data indicated the formation of 1:1 ligand:Fe complexes for the dithiosemicarbazones (**12** and **13**), while the dibenzoylpyridine ligands (**16a**–**e**) formed 2:1 ligand:Fe complexes. Therefore, together with their ability to mobilize intracellular Fe and prevent Fe uptake from Tf, the anti-proliferative activity of the novel chelators could be due, at least in part, to the formation of redox-active Fe complexes that generate cytotoxic ROS.

Structure–activity relationship analysis was performed in order to better understand the structural requirements needed for the dimeric thiosemicarbazones to exhibit biological activity. Of the novel chelators, the dithiosemicarbazone **12** and the 2,6-diBpT derivative **16a** showed the highest anti-proliferative activity. By examining the calculated partition coefficients of the synthesized compounds, it was shown that the most active chelator **16a** (R═H) had the lowest lipophilicity (log P_{calc} 3.8). On the other hand, the larger and more lipophilic chelators, namely **16e** (log P_{calc} = 8.17; 586 Da) and **13** (log P_{calc} = 9.19; 678 Da), showed reduced potency. When comparing the two dithiosemicarbazones, compound **13** (bearing a dodecane linker) was less effective than chelator **12** (which possessed a shorter hexane linker) in terms of chelation efficacy and inhibiting proliferation. Ligands with a high molecular weight and lipophilicity may not effectively permeate the cell membrane or may become trapped within the lipophilic environment of the membrane. This effect will prevent intracellular Fe chelation and decrease the formation of redox-active metal complexes within the cell that are necessary for their cytotoxic efficacy.

Overall, this investigation has demonstrated that the length of the hydrocarbon linker in dithiosemicarbazones and the nature of the substituents on dibenzoylpyridine-based thiosemicarbazones has a strong influence on their biological activity. Furthermore, the study has, for the first time, highlighted the potential of dimeric thiosemicarbazone compounds to act as selective Fe chelators for the treatment of cancer. Given that higher lipophilicity was detrimental towards dimer activity, future work could be directed towards synthesizing dithiosemicarbazones with shorter or more polar linkers and 2,6-diBpT analogs containing less hydrophobic substituents. Hence, this study highlights structure–activity relationships involved in the anti-proliferative activity and Fe chelation efficacy of thiosemicarbazone dimers and provides greater understanding towards the structural requirements for effective dimer design.

Abbreviations

Bp-1,6-hexanediT	2′-benzoylpyridine-(1,6-hexane)-dithiosemicarbazone
Bp-1,12-dodecanediT	2′-benzoylpyridine-(1,12-dodecane)-dithiosemicarbazone
Bp4aT	2′-benzoylpyridine 4-allyl-3-thiosemicarbazone
Bp4eT	2′-benzoylpyridine 4-ethyl-3-thiosemicarbazone
Bp44mT	2′-benzoylpyridine 4,4-dimethyl-3-thiosemicarbazone
Bp4mT	2′-benzoylpyridine 4-methyl-3-thiosemicarbazone
Bp4pT	2′-benzoylpyridine 4-phenyl-3-thiosemicarbazone
BpT	2′-benzoylpyridine thiosemicarbazone
DCM	dichloromethane
DFO	desferrioxamine
2,6-diBpT	2,6-dibenzoylpyridine thiosemicarbazone
2,6-diBp4aT	2,6-dibenzoylpyridine 4-allyl-3-thiosemicarbazone
2,6-diBp4eT	2,6-dibenzoylpyridine 4-ethyl-3-thiosemicarbazone
2,6-diBp4mT	2,6-dibenzoylpyridine 4-methyl-3-thiosemicarbazone
2,6-diBp4pT	2,6-dibenzoylpyridine 4-phenyl-3-thiosemicarbazone
Dp44mT	di-2-pyridylketone 4,4-dimethyl-3-thiosemicarbazone
ESI	electrospray ionization
HRMS	high-resolution mass spectrometry
NBpT	2′-(3-nitrobenzoyl)pyridine thiosemicarbazone
NDRG1	N-myc downstream regulated gene-1
NHE	normal hydrogen electrode
PBS	phosphate buffered saline
ROS	reactive oxygen species
RR	ribonucleotide reductase
Tf	transferrin
TMS	tetramethylsilane
XBpT	halogenated 2′-benzoylpyridine thiosemicarbazone

Acknowledgments

This work was supported by a Project Grant from the National Health and Medical Research Council (NHMRC) Australia to D.R.R. [Grant 632778]; and D.S.K. [Grant 1048972]; a NHMRC Senior Principal Research Fellowship to D.R.R. [Grant 571123]; a Cancer Institute New South Wales Early Career Development Fellowship to D.S.K. [Grant 08/ECF/1-30]; a Cancer Institute Research Innovation Grant to D.R.R. and D.S.K. [Grant 10/RFG/2-50]; and a Helen and Robert Ellis Fellowship to D.S.K. from the Sydney Medical School Foundation of The University of Sydney. The research was additionally supported by an ARC Discovery Grant (DP1095159) and Linkage Project Grant (LP110200635) to N.K. We kindly thank Dr. Mohan Bhadhade (Crystallography Laboratory, Analytical Centre, The University of New South Wales, Sydney, Australia) for collecting X-ray crystal structure data.

Appendix A. Supplementary data

Supplementary data to this article can be found online at http://dx.doi.org/10.1016/j.jinorgbio.2014.07.020. These data include MOL files and InChiKeys of the most important compounds described in this article.

References

[1] D.S. Kalinowski, D.R. Richardson, Pharmacol. Rev. 57 (2005) 547–583.
[2] A. Garoufis, S.K. Hadjikakou, N. Hadjiliadis, Coord. Chem. Rev. 253 (2009) 1384–1397.
[3] D.D. Perrin, H. Stünzi, Pharmacol. Ther. 12 (1981) 255–297.
[4] M. Aslantas, E. Kendi, N. Demir, A.E. Sabik, M. Tümer, M. Kertmen, Spectrochim. Acta A 74 (2009) 617–624.
[5] A.A. Al-Amiery, A.A.H. Kadhum, A.B. Mohamad, Bioinorg. Chem. Appl. (2012) 1–6.
[6] C.M. da Silva, D.L. da Silva, L.V. Modolo, R.B. Alves, M.A. de Resende, C.V.B. Martins, Â. de Fátima, J. Adv. Res. 2 (2011) 1–8.
[7] W.X. Hu, W. Zhou, C.N. Xia, X. Wen, Bioorg. Med. Chem. Lett. 16 (2006) 2213–2218.
[8] I. Đilovic, M. Rubcic, V. Vrdoljak, S.K. Pavelic, M. Kralj, I. Piantanida, M. Cindric, Bioorg. Med. Chem. 16 (2008) 5189–5198.
[9] D.S. Kalinowski, D.R. Richardson, Chem. Res. Toxicol. 20 (2007) 715–720.
[10] R. Setnescu, C. Barcutean, S. Jipa, T. Setnescu, M. Negoiu, I. Mihalcea, M. Dumitru, T. Zaharescu, Polym. Degrad. Stab. 85 (2004) 997–1001.
[11] G. Pelosi, Open Crystallogr. J. 3 (2010) 16–28.
[12] D.B. Lovejoy, P.J. Jansson, U.T. Brunk, J. Wong, P. Ponka, D.R. Richardson, Cancer Res. 71 (2011) 5871–5880.
[13] D.R. Richardson, P.C. Sharpe, D.B. Lovejoy, D. Senaratne, D.S. Kalinowski, M. Islam, P. V. Bernhardt, J. Med. Chem. 49 (2006) 6510–6521.
[14] J. Yuan, D.B. Lovejoy, D.R. Richardson, Blood 104 (2004) 1450–1458.
[15] D.R. Richardson, Crit. Rev. Oncol. Hematol. 42 (2002) 267–281.
[16] M.W. Hentze, M.U. Muckenthaler, N.C. Andrews, Cell 117 (2004) 285–297.
[17] P.T. Lieu, M. Heiskala, P.A. Peterson, Y. Yang, Mol. Aspects Med. 22 (2001) 1–87.
[18] I. De Domenico, D. McVey Ward, J. Kaplan, Nat. Rev. Mol. Cell Biol. 9 (2008) 72–81.
[19] N.T.V. Le, D.R. Richardson, Biochim. Biophys. Acta 1603 (2002) 31–46.

[20] A.M. Merlot, D.S. Kalinowski, D.R. Richardson, Antioxid. Redox Signal. 18 (2012) 973–1006.
[21] Y. Yu, D.S. Kalinowski, Z. Kovacevic, A.R. Siafakas, P.J. Jansson, C. Stefani, D.B. Lovejoy, P.C. Sharpe, P.V. Bernhardt, D.R. Richardson, J. Med. Chem. 52 (2009) 5271–5294.
[22] M. Kolberg, K.R. Strand, P. Graff, K. Kristoffer Andersson, Biochim. Biophys. Acta 1699 (2004) 1–34.
[23] C.E. Cooper, G.R. Lynagh, K.P. Hoyes, R.C. Hider, R. Cammack, J.B. Porter, J. Biol. Chem. 271 (1996) 20291–20299.
[24] N.T.V. Le, D.R. Richardson, Blood 104 (2004) 2967–2975.
[25] Z. Chen, D. Zhang, F. Yue, M. Zheng, Z. Kovacevic, D.R. Richardson, J. Biol. Chem. 287 (2012) 17016–17028.
[26] W. Liu, F. Xing, M. Iiizumi-Gairani, H. Okuda, M. Watabe, S.K. Pai, P.R. Pandey, S. Hirota, A. Kobayashi, Y.-Y. Mo, K. Fukuda, Y. Li, K. Watabe, EMBO Mol. Med. 4 (2012) 93–108.
[27] Z. Kovacevic, S. Chikhani, G.Y.L. Lui, S. Sivagurunathan, D.R. Richardson, Antioxid. Redox Signal. 18 (2013) 874–887.
[28] R.A. Finch, M.-C. Liu, A.H. Cory, J.G. Cory, A.C. Sartorelli, Adv. Enzym. Regul. 39 (1999) 3–12.
[29] R.A. Finch, M.-C. Liu, S.P. Grill, W.C. Rose, R. Loomis, K.M. Vasquez, Y.-C. Cheng, A.C. Sartorelli, Biochem. Pharmacol. 59 (2000) 983–991.
[30] S. Wadler, D. Makower, C. Clairmont, P. Lambert, K. Fehn, M. Sznol, J. Clin. Oncol. 22 (2004) 1553–1563.
[31] Y. Yen, K. Margolin, J. Doroshow, M. Fishman, B. Johnson, C. Clairmont, D. Sullivan, M. Sznol, Cancer Chemother. Pharmacol. 54 (2004) 331–342.
[32] C.A. Kunos, T. Radivoyevitch, S. Waggoner, R. Debernardo, K. Zanotti, K. Resnick, N. Fusco, R. Adams, R. Redline, P. Faulhaber, A. Dowlati, Gynecol. Oncol. 130 (2013) 75–80.
[33] D.S. Kalinowski, Y. Yu, P.C. Sharpe, M. Islam, Y.-T. Liao, D.B. Lovejoy, N. Kumar, P.V. Bernhardt, D.R. Richardson, J. Med. Chem. 50 (2007) 3716–3729.
[34] C. Stefani, G. Punnia-Moorthy, D.B. Lovejoy, P.J. Jansson, D.S. Kalinowski, P.C. Sharpe, P.V. Bernhardt, D.R. Richardson, J. Med. Chem. 54 (2011) 6936–6948.
[35] Y. Yu, Y.S. Rahmanto, D.R. Richardson, Br. J. Pharmacol. 165 (2012) 148–166.
[36] A.Y. Lukmantara, D.S. Kalinowski, N. Kumar, D.R. Richardson, Bioorg. Med. Chem. Lett. 23 (2013) 967–974.
[37] A.Y. Lukmantara, D.S. Kalinowski, N. Kumar, D.R. Richardson, Org. Biomol. Chem. 11 (2013) 6414–6425.
[38] Y.F. Han, C.P.L. Li, E. Chow, H. Wang, Y.-P. Pang, P.R. Carlier, Bioorg. Med. Chem. 7 (1999) 2569–2575.
[39] M. Sarkis, D.N. Tran, S. Kolb, M.A. Miteva, B.O. Villoutreix, C. Garbay, E. Braud, Bioorg. Med. Chem. Lett. 22 (2012) 7345–7350.
[40] O.P. Pandey, S.K. Sengupta, M.K. Mishra, C.M. Tripathi, Bioinorg. Chem. Appl. 1 (2003) 35–44.
[41] T. Stringer, P. Chellan, B. Therrien, N. Shunmoogam-Gounden, D.T. Hendricks, G.S. Smith, Polyhedron 28 (2009) 2839–2846.
[42] J.K. Swearingen, D.X. West, Transit. Met. Chem. 25 (2000) 241–246.
[43] H.G. Petering, H.H. Buskirk, G.E. Underwood, Cancer Res. 24 (1964) 367–372.
[44] D.X. West, J.S. Ives, G.A. Bain, A.E. Liberta, J. Valdés-Martínez, K.H. Ebert, S. Hernández-Ortega, Polyhedron 16 (1997) 1895–1905.
[45] H. Beraldo, D.X. West, Transit. Met. Chem. 22 (1997) 294–298.
[46] P.J. Blower, J.S. Lewis, J. Zweit, Nucl. Med. Biol. 23 (1996) 957–980.
[47] M. Christlieb, H.S.R. Struthers, P.D. Bonnitcha, A.R. Cowley, J.R. Dilworth, Dalton Trans. (2007) 5043–5054.
[48] A. Kanchana Devi, R. Ramesh, Spectrochim. Acta A 117 (2014) 138–143.
[49] B.M. Paterson, P.S. Donnelly, Chem. Soc. Rev. 40 (2011) 3005–3018.
[50] G.J. Van Glessen, J.A. Crim, D.H. Petering, H.G. Petering, J. Natl. Cancer Inst. 51 (1973) 139–146.
[51] A. Castiñeiras, E. Bermejo, D.X. West, L.J. Ackerman, J. Valdés-Martínez, S. Hernández-Ortega, Polyhedron 18 (1999) 1463–1469.
[52] A. Castiñeiras, E. Bermejo, D.X. West, A.K. El-Sawaf, J.K. Swearingen, Polyhedron 17 (1998) 2751–2757.
[53] A.I. Matesanz, J.M. Pérez, P. Navarro, J.M. Moreno, E. Colacio, P. Souza, J. Inorg. Biochem. 76 (1999) 29–37.
[54] E. López-Torres, M.A. Mendiola, Inorg. Chim. Acta 363 (2010) 1735–1740.
[55] B.A. Gingras, T. Suprunchuk, C.H. Bayley, Can. J. Chem. 40 (1962) 1053–1059.
[56] D.M. Wiles, B.A. Gingras, T. Suprunchuk, Can. J. Chem. 45 (1967) 1735–1743.
[57] Bruker, SADABS, Bruker AXS Inc., Madison, Wisconsin, USA, 2001.
[58] Bruker, APEX2 and SAINT, Bruker AXS Inc., Madison, Wisconsin, USA, 2001.
[59] G.M. Sheldrick, Acta Crystallogr. A64 (2008) 112–122.
[60] C.F. Macrae, I.J. Bruno, J.A. Chisholm, P.R. Edgington, P. McCabe, E. Pidcock, L. Rodriguez-Monge, R. Taylor, J. van de Streek, P.A. Wood, J. Appl. Crystallogr. 41 (2008) 466–470.
[61] D. Richardson, E. Tran, P. Ponka, Blood 86 (1995) 4295–4306.
[62] D.R. Richardson, E. Baker, J. Biol. Chem. 267 (1992) 21384–21389.
[63] D.R. Richardson, E. Baker, Biochim. Biophys. Acta 1053 (1990) 1–12.
[64] T.D. Lash, K. Pokharel, J.M. Serling, V.R. Yant, G.M. Ferrence, Org. Lett. 9 (2007) 2863–2866.
[65] B.X. Hu, Z.L. Shen, J. Lu, X.Q. Hu, W.M. Mo, N. Sun, D. Xu, Phosphorus Sulfur 184 (2009) 523–535.
[66] P.V. Bernhardt, J. Mattsson, D.R. Richardson, Inorg. Chem. 45 (2006) 752–760.
[67] M. Whitnall, J. Howard, P. Ponka, D.R. Richardson, Proc. Natl. Acad. Sci. U. S. A. 103 (2006) 14901–14906.
[68] D.S. Kalinowski, P.C. Sharpe, P.V. Bernhardt, D.R. Richardson, J. Med. Chem. 51 (2007) 331–344.
[69] D.B. Lovejoy, D.M. Sharp, N. Seebacher, P. Obeidy, T. Prichard, C. Stefani, M.T. Basha, P.C. Sharpe, P.J. Jansson, D.S. Kalinowski, P.V. Bernhardt, D.R. Richardson, J. Med. Chem. 55 (2012) 7230–7244.
[70] D.R. Richardson, K. Milnes, Blood 89 (1997) 3025–3038.
[71] J.T. Edward, P. Ponka, D.R. Richardson, Biometals 8 (1995) 209–217.